

Electronic Structure of Bis(imino)pyridine Iron Dichloride, Monochloride, and Neutral Ligand Complexes: A Combined Structural, Spectroscopic, and Computational Study

Suzanne C. Bart,[†] Krzysztof Chłopek,[‡] Eckhard Bill,[‡] Marco W. Bouwkamp,[†]
Emil Lobkovsky,[†] Frank Neese,^{*,‡,§} Karl Wieghardt,^{*,‡} and Paul J. Chirik^{*,†}

*Contribution from the Department of Chemistry and Chemical Biology, Baker Laboratory,
Cornell University, Ithaca, New York 14853, and Max-Planck Institute of Bioinorganic
Chemistry, Stiftstrasse 34-36, D-45470 Mülheim an der Ruhr, Germany*

Received June 27, 2006; E-mail: pc92@cornell.edu

Abstract: The electronic structure of a family of bis(imino)pyridine iron dihalide, monohalide, and neutral ligand compounds has been investigated by spectroscopic and computational methods. The metrical parameters combined with Mössbauer spectroscopic and magnetic data for (PrPDI)FeCl₂ (PrPDI = 2,6-(2,6-Pr₂C₆H₃N=CMe)₂C₅H₃N) established a high-spin ferrous center ligated by a neutral bis(imino)pyridine ligand. Comparing these data to those for the single electron reduction product, (PrPDI)FeCl, again demonstrated a high-spin ferrous ion, but in this case the S_{Fe} = 2 metal center is antiferromagnetically coupled to a ligand-centered radical (S_L = 1/2), accounting for the experimentally observed S = 3/2 ground state. Continued reduction to (PrPDI)FeL_n (L = N₂, n = 1, 2; CO, n = 2; 4-(N,N-dimethylamino)pyridine, n = 1) resulted in a doubly reduced bis(imino)pyridine diradical, preserving the ferrous ion. Both the computational and the experimental data for the N,N-(dimethylamino)pyridine compound demonstrate nearly isoenergetic singlet (S_L = 0) and triplet (S_L = 1) forms of the bis(imino)pyridine dianion. In both spin states, the iron is intermediate spin (S_{Fe} = 1) ferrous. Experimentally, the compound has a spin singlet ground state (S = 0) due to antiferromagnetic coupling of iron and the ligand triplet state. Mixing of the singlet diradical excited state with the triplet ground state of the ligand via spin–orbit coupling results in temperature-independent paramagnetism and accounts for the large dispersion in ¹H NMR chemical shifts observed for the in-plane protons on the chelate. Overall, these studies establish that reduction of (PrPDI)FeCl₂ with alkali metal or borohydride reagents results in sequential electron transfers to the conjugated π-system of the ligand rather than to the metal center.

Introduction

Aryl-substituted bis(imino)pyridines, [2,6-(ArN=CMe)₂C₅H₃N] (Ar = substituted aryl group),¹ have emerged as a prominent class of ligands due to their ease of synthesis, steric and electronic modularity, and ability to stabilize a range of transition metal and alkali metal ions.² These terdentate chelates have special relevance in iron chemistry, supporting highly active catalysts for ethylene and α-olefin polymerization upon treatment of the ferrous precursor with an appropriate activator.^{3,4} More recently, reduced versions of these compounds have been used in catalytic transformations including olefin and alkyne hydrogenation and hydrosilylation.⁵

Inspiration for the design of catalysts for the latter class of reactions was provided by the seminal work of Wrighton and co-workers, who described the photocatalytic hydrogenation, hydrosilylation, and isomerization of unactivated olefins with

Fe(CO)₅ irradiated with 366 nm light.^{6,7} Because photogenerated [Fe(CO)₃] is proposed as the active species, we reasoned that introduction of a terdentate bis(imino)pyridine chelate may allow thermal access to a catalytically active [(PrPDI)Fe] (PrPDI = 2,6-(2,6-Pr₂C₆H₃N=CMe)₂C₅H₃N) fragment. Sodium amalgam reduction of the ferrous dihalide complexes, (PrPDI)FeX₂ (X = Cl, 1-Cl₂; Br, 1-Br₂), furnished an unusual iron bis(dinitrogen) complex, (PrPDI)Fe(N₂)₂ (1-(N₂)₂) (Figure 1).⁵ During the

- (3) (a) Small, B. L.; Brookhart, M.; Bennett, A. M. *J. Am. Chem. Soc.* **1998**, *120*, 4049. (b) Britovsek, G. J. P.; Gibson, V. C.; Kimberley, B. S.; Maddox, P. J.; McTavish, S. J.; Solan, G. A.; White, A. J. P.; Williams, D. J. *Chem. Commun.* **1998**, 849. (c) Britovsek, G. J. P.; Bruce, M.; Gibson, V. C.; Kimberley, B. S.; Maddox, P. J.; Mastroianni, S.; McTavish, S. J.; Redshaw, C.; Solan, G. A.; Strömberg, S.; White, A. J. P.; Williams, D. J. *J. Am. Chem. Soc.* **1999**, *121*, 8728. (d) Gibson, V. C.; Spitzmesser, S. K. *Chem. Rev.* **2003**, *103*, 283. (e) Bianchini, C.; Mantovani, G.; Meli, A.; Migliacci, D.; Zanobini, F.; Laschi, F.; Sommazzi, A. *Eur. J. Inorg. Chem.* **2003**, 1620. (f) Bouwkamp, M. W.; Lobkovsky, E.; Chirik, P. J. *J. Am. Chem. Soc.* **2005**, *127*, 9660.
- (4) Bianchini, C.; Giambastiani, G.; Rios, I. G.; Mantovani, G.; Meli, A.; Segarra, A. M. *Coord. Chem. Rev.* **2006**, *250*, 1391.
- (5) Bart, S. C.; Lobkovsky, E.; Chirik, P. J. *J. Am. Chem. Soc.* **2004**, *126*, 13794.
- (6) (a) Schroeder, M. A.; Wrighton, M. S. *J. Am. Chem. Soc.* **1976**, *98*, 551. (b) Schroeder, M. A.; Wrighton, M. S. *J. Organomet. Chem.* **1977**, *128*, 345.
- (7) For a recent computational study on Fe(CO)₅ photocatalyzed olefin hydrogenation reactions, see: Kismartoni, L. C.; Weitz, E.; Cedeno, D. L. *Organometallics* **2005**, *24*, 4714.

[†] Cornell University.

[‡] Max-Planck Institute of Bioinorganic Chemistry.

[§] Present address: Institut für Physikalische und Theoretische Chemie, Universität Bonn, Wegelerstrasse 12, D-53115 Bonn, Germany.

(1) Ittel, S. D.; Johnson, L. K.; Brookhart, M. *Chem. Rev.* **2000**, *100*, 1169.

(2) Blackmore, I. J.; Gibson, V. C.; Hitchcock, P. B.; Rees, C. W.; Williams, D. J.; White, A. J. P. *J. Am. Chem. Soc.* **2005**, *127*, 6012.

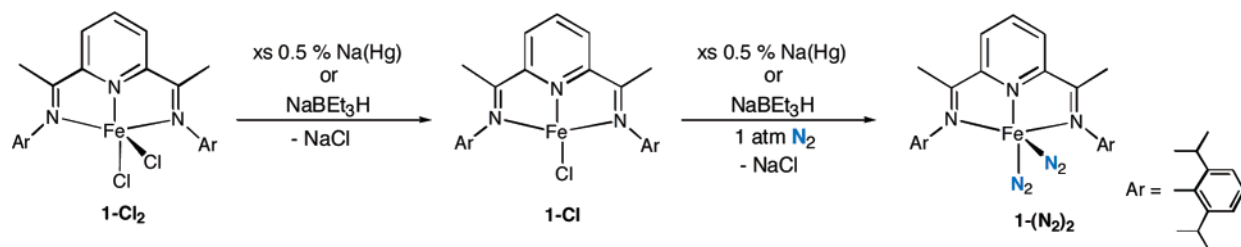


Figure 1. Reduction of (iPrPDI)FeCl₂ (**1-Cl₂**).

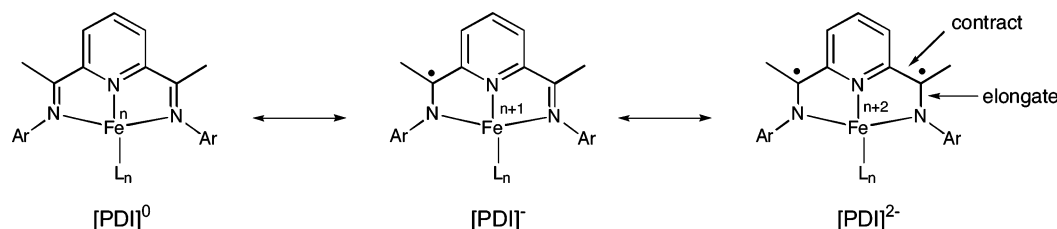


Figure 2. Redox activity of bis(imino)pyridine ligands in iron coordination compounds.

course of the reduction reaction, intermediate four-coordinate iron monohalide compounds, (iPrPDI)FeX (X = Cl, **1-Cl**; Br, **1-Br**), were isolated and found to have quartet ($S = 3/2$) ground states.⁸ Notably, **1-(N₂)₂** is an effective precatalyst for the hydrogenation and hydrosilation of olefins with synthetically useful turnover frequencies at part per million catalyst loadings in nonpolar media.⁵

One intriguing feature of **1-(N₂)₂** is its NMR spectrum, where resonances are observed over a 15 ppm chemical shift range. Salient features include observation of an imine methyl group centered at 13.61 ppm and a *p*-pyridine resonance at 2.58 ppm (benzene-*d*₆, 23 °C, 1 atm N₂). These observations suggest energetically accessible $S = 1$ states, an unexpected electronic configuration for an iron(0) center. While high-spin d⁸ complexes have been reported for nickel(II),⁹ an isoelectronic $S = 1$ iron species is to our knowledge unknown. Typically iron(0) complexes such as Fe(CO)₅ are diamagnetic, a consequence of a large crystal field stabilization energy imparted by the strong field ligands. The unusual electronic structure of **1-(N₂)₂** is further highlighted when compared to a similar, iron bis-(dinitrogen) complex reported by Danopoulos and co-workers, where the imine donors have been replaced by *N*-heterocyclic carbenes.¹⁰

These observations suggest that the bis(imino)pyridine ligand is responsible for the unusual properties of **1-(N₂)₂**. It is now well-established that chelates of this type are both chemically^{2a,11–17} and redox active,^{18–22} potentially accepting up to

three electrons in the conjugated π -system.²² The ability of bis-(imino)pyridines to serve as electron reservoirs may ultimately prove useful in designing new catalysts or reagents for small molecule activation.²³ In this manuscript, we report a combined structural, spectroscopic, and computational study aimed at exploring the electronic structure of reduced bis(imino)pyridine iron compounds. The results highlight the ability of the terdentate ligand to accept electron density from the iron and stabilize unusual monohalide and neutral ligand compounds.

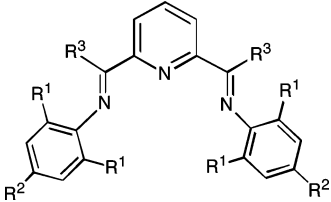
Results and Discussion

General Approach. Several parameters were evaluated to determine the degree of bis(imino)pyridine ligand participation in the electronic structure of the reduced iron complexes, **1-Cl** and **1-(N₂)₂**. As described previously,^{18–21} the metrical parameters of high-quality X-ray crystal structures are indicative of ligand-centered radicals. Specifically, reduction of the terdentate chelate populates molecular orbitals of the bis(imino)pyridine fragment that are antibonding with respect to the imine but bonding with respect to the carbon backbone. As a consequence, the N_{imine}–C_{imine} bonds elongate while the C_{imine}–C_{ipso} distances contract (Figure 2). In addition to structural data, magnetic studies and Mössbauer spectroscopy also provide experimental insight into the electronic structure of the complexes. The experimental studies have been conducted in parallel with DFT calculations to arrive at an experimentally calibrated bonding picture. As described previously,²⁴ the theoretical work and hence view of the electronic structure is validated by the capability to predict both spectroscopic and metrical parameters.²⁵

Reference Compounds. To assign the oxidation states of both the ligand and the metal in the products of **1-Cl₂** reduction, a series of reference compounds were initially studied to

- (8) Bouwkamp, M. W.; Bart, S. C.; Hawrelak, E. J.; Trovitch, R. J.; Lobkovsky, E.; Chirik, P. J. *Chem. Commun.* **2005**, 3406.
- (9) Furlani, C. *Coord. Chem. Rev.* **1968**, 3, 141.
- (10) Danopoulos, A. A.; Wright, J. A.; Motherwell, W. B. *Chem. Commun.* **2005**, 784.
- (11) Bouwkamp, M. W.; Lobkovsky, E.; Chirik, P. J. *Inorg. Chem.* **2006**, 45, 2.
- (12) Sugiyama, I.; Korobkov, S.; Gambarotta, S.; Mueller, A.; Budzelaar, P. H. M. *Inorg. Chem.* **2004**, 43, 5771.
- (13) Scott, J.; Gambarotta, S.; Korobkov, I.; Budzelaar, P. H. M. *J. Am. Chem. Soc.* **2005**, 127, 13019.
- (14) Kooistra, T. K.; Hettterscheid, D. G. H.; Schwartz, E.; Knijnenburg, Q.; Budzelaar, P. H. M.; Gal, A. W. *Inorg. Chim. Acta* **2004**, 357, 2945.
- (15) Sugiyama, H.; Aharonian, G.; Gambarotta, S.; Yap, G. P. A.; Budzelaar, P. H. M. *J. Am. Chem. Soc.* **2002**, 124, 12268.
- (16) Reardon, D.; Conan, F.; Gambarotta, S.; Yap, G.; Wang, Q. Y. *J. Am. Chem. Soc.* **1999**, 121, 9318.
- (17) Bruce, M.; Gibson, V. C.; Redshaw, C.; Solan, G. A.; White, A. J. P.; Williams, D. J. *Chem. Commun.* **1998**, 2523.
- (18) de Bruin, B.; Bill, E.; Bothe, E.; Weyhermüller, T.; Wieghardt, K. *Inorg. Chem.* **2000**, 39, 2936.

- (19) Budzelaar, P. H. M.; de Bruin, B.; Gal, A. W.; Wieghardt, K.; van Lenthe, J. H. *Inorg. Chem.* **2001**, 40, 4649.
- (20) Scott, J.; Gambarotta, S.; Korobkov, I.; Knijnenburg, Q.; de Bruin, B.; Budzelaar, P. H. M. *J. Am. Chem. Soc.* **2005**, 127, 17204.
- (21) Scott, J.; Gambarotta, S.; Korobkov, I.; Budzelaar, P. H. M. *Organometallics* **2005**, 24, 6298.
- (22) Enright, D.; Gambarotta, S.; Yap, G. P. A.; Budzelaar, P. H. M. *Angew. Chem., Int. Ed.* **2002**, 41, 3873.
- (23) Scott, J.; Gambarotta, S.; Korobkov, I. *Can. J. Chem.* **2005**, 83, 279.
- (24) Ghosh, P.; Bill, E.; Weyhermüller, T.; Neese, F.; Wieghardt, K. *J. Am. Chem. Soc.* **2003**, 125, 1293.
- (25) Neese, F. *Inorg. Chim. Acta* **2002**, 337, 181.

Table 1. Selected Bond Distances for Crystallographically Characterized Aryl-Substituted Bis(imino)pyridines


R ¹	R ²	R ³	N _{imine} –C _{imine}	C _{imine} –C _{ipso}	C _{ipso} –N _{pyridine}	reference ^a
ⁱ Pr	H	Me	1.274(3)	1.489(3)	1.342(3)	this work
			1.274(3)	1.487(3)	1.345(3)	
ⁱ Pr	H	Me	1.266(6)	1.485(6)	1.345(6)	1
			1.273(5)	1.489(6)	1.356(5)	
Br	H	Me	1.284(8)	1.476(9)	1.354(8)	2
			1.261(8)	1.419(9)	1.341(8)	
H	OH	H	1.259(4)	1.464(4)	1.341(4)	3
			1.275(4)	1.466(4)	1.347(3)	
H	H	Me	1.266(5)	1.498(5)	1.340(4)	4
H	OMe	Me	1.274(4)	1.501(5)	1.343(4)	5
ⁱ Pr ^b	H	Me	1.284(3)	1.491(4)	1.349(3)	6
^t Bu, H			1.272(3)	1.495(4)	1.342(2)	
		average	1.271(17)	1.480(19)	1.345(17)	

^a (1) Yap, G. P. A.; Gambarotta, S. *CCDC* 151767. (2) Chen, Y.; Chen, R.; Qian, R.; Dong, X.; Sun, J. *Organometallics* **2003**, *23*, 4312. (3) Vance, A. L.; Alcock, N. W.; Heppert, J. A.; Busch, D. H. *Inorg. Chem.* **1998**, *37*, 6912. (4) Mentes, A.; Fawcett, J.; Kemmitt, R. D. W. *Acta Crystallogr., Sect. E* **2001**, *57*, 424. (5) Meehan, P. R.; Alyea, E. C.; Ferguson, G. *Acta Crystallogr., Sect. C* **1997**, *53*, 888. (6) Small, B. L.; Brookhart, M. *Macromolecules* **1999**, *32*, 2120. ^b 2-(2,6-ⁱPr₂-C₆H₃N=C(Me)), 6-(2-^tBu-C₆H₄NC)C₅H₃N.

calibrate the employed experimental and computational methodology. Initially, the free ligands were chosen because the bis(imino)pyridines are undoubtedly in the neutral form and will provide reference values for comparison with the iron complexes of interest.

Compiled in Table 1 are selected bond distances for crystallographically characterized aryl-substituted bis(imino)pyridine ligands obtained from either the Cambridge Structural Database²⁶ or data collected in our laboratory. As expected for a neutral bis(imino)pyridine, the average imine bond distance (N_{imine}–C_{imine}) of 1.271 Å is in the expected range for nitrogen–carbon double bonds. Likewise, the average C_{imine}–C_{ipso} bond length of 1.480 Å is in the typical range for carbon–carbon single bonds.

Computational studies on the metal-free species were initially conducted with *ab initio* methods, as this approach provides access to genuine multiconfigurational wave functions. The geometries were optimized at the SCF level (RHF or CASSCF depending on the context), and differential dynamic correlation was included with the iterative difference dedicated CI (IDDCI3) method.²⁷ The *ab initio* calculations serve as reference for the more approximate DFT methods that were used in the bulk of this work as they are computationally much more feasible as compared to the expensive multireference *ab initio* methods. In this case, one has to resort to broken symmetry techniques to arrive at realistic results for spin-coupled systems.²⁸ Because several broken symmetry solutions to the spin-unrestricted Kohn–Sham equations may be obtained for many of the compounds in this work, a general notation has been adopted. For this purpose, the systems have been divided into two fragments. The BS(*m,n*) descriptor refers to a broken symmetry state with *m* unpaired spin-up electrons on fragment 1 and *n* unpaired spin-down electrons essentially localized on fragment

2. In general, fragment 1 will correspond to the metal (zinc or iron) and fragment 2 will be the bis(imino)pyridine chelate. Note that in this notation a standard high-spin open-shell solution will be written as BS(*m+n*,0). The variational process does, however, have the freedom to converge to a solution of the form BS(*m–n*,0), where effectively the *n*-spin-down electrons pair with *n* < *m* spin-up electrons on the partner fragment. Such a solution is then a standard $M_S \cong S = (m-n)/2$ unrestricted Kohn–Sham solution. As explained in detail elsewhere,^{27–29} the nature of the solution is investigated by the corresponding orbital transformation, which, via the corresponding orbital overlaps, demonstrates whether the system is to be described as a spin-coupled or a closed-shell solution.

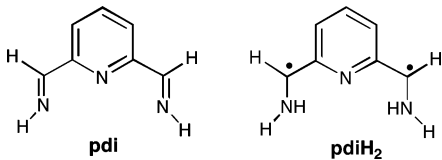
Two model compounds for the free bis(imino)pyridine were computationally investigated (Table 2). The first is a truncated form of the neutral ligand, 2,6-(HN=C(H))₂(C₅H₃N) (**pdi**), where both the imine aryl-substituents and the backbone methyl groups were replaced with hydrogen atoms. The computed (RHF) N_{imine}–C_{imine} and C_{imine}–C_{ipso} bond distances of 1.249 and 1.492 Å, respectively, are in good agreement with the experimentally determined average values of 1.271 and 1.480 Å (Table 1). A truncated form of a two electron reduced bis(imino)pyridine, 2,6-(H₂NC(H))₂(C₅H₃N) (**pdi-H₂**), was also studied computationally. Two hydrogen atoms were attached to the imine nitrogen atoms to maintain charge neutrality. To properly describe the diradical character of such a species, the most elementary approach possible is a multiconfigurational

(26) (a) Cambridge Structural Database Version 5.27. (b) ⁱPrPDI has been previously crystallized, and its structure was determined by X-ray diffraction: Yap, G. P. A.; Gambarotta, S. *CCDC* 151767.

(27) Miralles, J.; Daudey, J. P.; Caballol, R. *Chem. Phys. Lett.* **1992**, *198*, 555.

(28) (a) Calzado, C. J.; Sanz, J. F.; Malrieu, J. P.; Illas, F. *Chem. Phys. Lett.* **1999**, *307*, 102. (b) Calzado, C. J.; Malrieu, J. P. *Chem. Phys. Lett.* **2000**, *317*, 404. (c) Calzado, C. J.; Sanz, J. F.; Malrieu, J. P. *J. Chem. Phys.* **2000**, *112*, 5158. (d) Calzado, C. J.; Cabrero, J.; Malrieu, J. P.; Caballol, R. *J. Chem. Phys.* **2002**, *116*, 2728. (e) Calzado, C. J.; Cabrero, J.; Malrieu, J. P.; Caballol, R. *J. Chem. Phys.* **2002**, *116*, 3985. (f) Castell, O.; Caballol, R. *Inorg. Chem.* **1999**, *38*, 668. (g) Ray, K.; Weyhermüller, T.; Neese, F.; Wieghardt, K. *Inorg. Chem.* **2005**, *44*, 5345. (h) Ray, K.; Weyhermüller, T.; Neese, F.; Wieghardt, K. *Inorg. Chem.* **2005**, *44*, 3636. (i) Bill, E.; Bothe, E.; Chaudhuri, P.; Chlopek, K.; Herebian, D.; Kokatam, S.; Ray, K.; Weyhermüller, T.; Neese, F.; Wieghardt, K. *Chem. Eur. J.* **2004**, *11*, 204.

(29) Neese, F. *J. Phys. Chem. Solids* **2004**, *65*, 781.

Table 2. CASSCF Computed Bond Distances for **pdi** and **pdi-H₂**


N _{imine} –C _{imine}	1.249	1.363
C _{imine} –C _{ipso}	1.492	1.443
C _{ipso} –N _{pyridine}	1.317	1.332

wave function with two electrons in two active orbitals (referred to as CASSCF(2,2)). As expected, the CASSCF(2,2) optimized geometry shows that the N_{imine}–C_{imine} distances lengthen to 1.363 Å while the C_{imine}–C_{ipso} bonds contract to 1.443 Å. At the CASSCF(2,2) or the IDDCI3(2,2) level, **pdi-H₂** is predicted to be a ground-state triplet with the singlet state ~1500 cm^{−1} (4.3 kcal/mol) higher in energy. DFT calculations reveal the same trend with an attenuated energy gap where the singlet state lies 725 cm^{−1} (2.3 kcal/mol) above the triplet using the broken symmetry strategy. These results do not necessarily imply preferential ligand coordination in the triplet state but rather that both multiplicities are energetically accessible.

The geometric changes observed upon reduction of **pdi** to **pdi-H₂** are readily understood from examination of the frontier molecular orbitals. The SOMOs (Figure 3) of **pdi-H₂** are unoccupied in **pdi** and are antibonding with respect to the imine and bonding with respect to the C_{imine}–C_{ipso}. Thus, one or two electron occupation of these orbitals produces the geometric changes computed for ligand reduction (Figure 2).

Having explored the electronic structure of the free ligand and its corresponding dianion, a series of hypothetical bis(imino)pyridine zinc(II) 4-(*N,N*-dimethylamino)pyridine model complexes ([(^{Me}**pdi**)Zn(DMAP)]ⁿ⁺ (*n* = 0, 1, 2, ^{Me}**pdi** = 2,6-(MeN=C(Me))₂(C₅H₃N))) was also investigated. As previous work has demonstrated,¹⁸ the closed-shell, d¹⁰ Zn(II) ion does not engage in redox chemistry with the ligand, and therefore reductions are ligand rather than metal-based and can be systematically studied. As a result, the computed N_{imine}–C_{imine} and C_{imine}–C_{ipso} bond distances for the neutral, cationic, and dicationic zinc complexes will provide a foundation for the neutral, one, and two electron reduced forms of a coordinated bis(imino)pyridine ligand.

Presented in Table 3 are selected metrical data for the zinc compounds from the broken symmetry computations using the B3LYP functional. As expected for a Zn(II) complex, five doubly occupied metal orbitals were located that are very low in energy relative to the PDI π -system, supporting the idea that all of the redox chemistry is indeed ligand centered. Diamagnetic [(^{Me}**pdi**)Zn(DMAP)]²⁺ has optimized N_{imine}–C_{imine} and C_{imine}–C_{ipso} bond lengths of 1.30 and 1.51 Å, consistent with a neutral closed-shell [PDI]⁰ ligand. One electron reduction to yield [(^{Me}**pdi**)Zn(DMAP)]⁺ resulted in a contraction of the C_{imine}–C_{ipso} distances to 1.47 Å and elongation of N_{imine}–C_{imine} to 1.33 Å, consistent with the experimental values for a paramagnetic aluminum complex where the PDI ligand was reduced by one electron.²⁰ The SOMO (Figure 4a) is principally ligand centered and resembles the b₂ ligand orbital computed for **pdi-H₂**. Thus, [(^{Me}**pdi**)Zn(DMAP)]⁺ is best described as a Zn(II) complex with a monoanionic bis(imino)pyridine ligand with a π -centered radical (*S*_L = 1/2). A total spin-density plot is presented in Figure S1 of the Supporting Information.

Two electron reduction of the hypothetical zinc compound produced neutral (^{Me}**pdi**)Zn(DMAP), where the PDI ligand undergoes further bond length distortions. The optimized values (BP86 functional) in the diamagnetic zinc compound are in agreement with those calculated for **pdi-H₂**, consistent with a two electron reduction of the bis(imino)pyridine ligand. The computed HOMO of (^{Me}**pdi**)Zn(DMAP) (Figure 4b) is reminiscent of the b₂ SOMO of **pdi-H₂** (Figure 3) with an additional minor Zn-4p contribution that is antibonding with respect to the bis(imino)pyridine ligand. A separate analysis of (^{Me}**pdi**)-Zn(DMAP) with the hybrid B3LYP functional also revealed a broken symmetry solution with the two SOMOs containing “spin-up” and “spin-down” electrons in principally ligand-based orbitals. The diradical adopts a preferentially antiparallel alignment. The spatial overlap of the two corresponding SOMOs is *S* = 0.69.²⁹ Note values of *S* approaching 1.0 indicate a standard doubly populated molecular orbital with little spin polarization, while values of *S* \ll 1 indicate nonorthogonal magnetic orbital pairs. For (^{Me}**pdi**)Zn(DMAP), the spatial overlap of the SOMOs is consistent with strong antiferromagnetic coupling. Calculation of the exchange coupling constant, *J*, using the Yamaguchi approach³⁰ produced a value of −970 cm^{−1}. Therefore, (^{Me}**pdi**)-Zn(DMAP) is best described as a Zn(II) ion containing a singlet diradical bis(imino)pyridine ligand, where the unpaired spins couple through a zinc-based 4p-orbital.

Unfortunately, all of our attempts to verify the computational predictions experimentally by preparation of (ⁱPrPDI)Zn(DMAP) have been unsuccessful. Stirring (ⁱPrPDI)ZnCl₂³¹ with a host of reductants (Sn, Mg, 0.5% Na(Hg), NaBEt₃H) in the presence of DMAP or pyridine (0.5% Na(Hg) only) produced an intractable mixture of compounds. Alternative synthetic routes such as treatment of (DMAP)₂ZnCl₂ and py₂ZnCl₂³² with ⁱPrPDI and Mg were also unsuccessful.

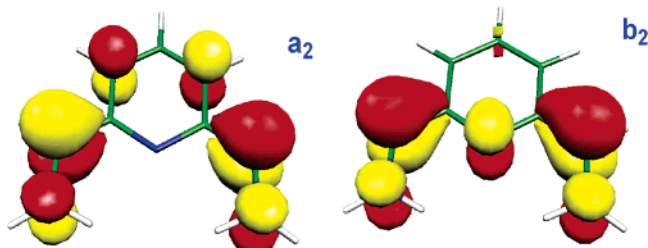
Bis(imino)pyridine Iron Complexes: (ⁱPrPDI)FeCl₂ (1-Cl₂). With reference values for mono- and direduced forms of the bis(imino)pyridine ligands established, the experimental X-ray crystallographic, magnetic, and Mössbauer spectroscopic parameters were determined for a family of iron compounds. As reported by Brookhart and Gibson,^{3a,b} **1-Cl₂** is a five-coordinate complex with a quintet ground state. The previously reported metrical data reveal N_{imine}–C_{imine} distances of 1.301(7) Å and C_{imine}–C_{ipso} bond lengths of 1.482(8) Å, both consistent with the values established above for a neutral, [PDI]⁰ ligand coordinated to a high-spin, *S* = 2, ferrous ion. Gibson and co-workers³³ have previously reported the ambient temperature Mössbauer parameters for (^{Me}**pdi**)FeCl₂ (^{Me}**pdi** = 2,6-(2,4,6-Me₃C₆H₂N=CMe)₂C₅H₃N) and obtained an isomer shift of 0.90 mm/s and a quadrupole splitting of 1.12 mm/s. The parameters for **1-Cl₂** collected at 80 K reveal a similar isomer shift of 0.89 mm/s but a larger quadrupole splitting of 2.40 mm/s, fully consistent with high-spin iron(II).

(ⁱPrPDI)FeCl (1-Cl). As reported previously⁸ and highlighted in Figure 1, addition of various reducing agents to **1-Cl₂**

- (30) (a) Soda, T.; Kitagawa, Y.; Onishi, T.; Takano, Y.; Shigeta, T.; Nagao, H.; Yoshioka, Y.; Yamaguchi, K. *Chem. Phys. Lett.* **2000**, *319*, 233. (b) Yamaguchi, K.; Takahara, Y.; Fueno, T. In *Applied Quantum Chemistry*; Smith, V. H., Ed.; Reidel: Dordrecht, 1986; p 155. (c) Blanchard, S.; Neese, F.; Bothe, E.; Bill, E.; Weyermüller, T.; Wieghardt, K. *Inorg. Chem.* **2005**, *44*, 3636. (d) Chlopek, K.; Bothe, E.; Neese, F.; Weyhermüller, T.; Wieghardt, K. *Inorg. Chem.* **2006**, *45*, 6298.
- (31) Fan, R.; Zhu, D.; Ding, H.; Mu, Y.; Su, Q.; Xia, H. *Synth. Met.* **2005**, *149*, 135.
- (32) Graddon, D. P.; Heng, K. B.; Watton, E. C. *Aust. J. Chem.* **1966**, *19*, 1801.
- (33) Britovsek, G. J. P.; Clentsmith, G. K. B.; Gibson, V. C.; Goodgame, D. M. L.; McTavish, S. J.; Pankhurst, Q. A. *Catal. Commun.* **2002**, *3*, 207.

Table 3. Selected Bond Distances Arising from Broken Symmetry DFT Calculations for a Series of $[(^{\text{Me}}\text{pdi})\text{Zn}(\text{DMAP})]^{n+}$ Compounds

	$[\text{PDI}]^0$	$[\text{PDI}]^-$	$[\text{PDI}]^{2-}$
Nimine–Cimine	1.301	1.329	1.354
Cimine–Cipso	1.507	1.469	1.444
Cipso–Npyridine	1.344	1.368	1.387

**Figure 3.** Singly occupied molecular orbitals (SOMOs) of **pdi-H₂** from ab initio CASSCF(2,2) calculations with symmetry designations from the C_{2v} point group.

furnished the four-coordinate monochloride compound, **1-Cl**, with an ambient temperature benzene- d_6 solution magnetic moment of $3.7 \mu_B$, consistent with a quartet ($S = 3/2$) ground state. The electronic structure of **1-Cl** was studied computationally using the truncated compound, $(^{\text{Me}}\text{pdi})\text{FeCl}$, where the isopropyl aryl groups were replaced with methyl substituents. To find the correct electronic structure description, B3LYP calculations were carried out with the BS(4,1) and BS(3,0) schemes and produced distinct solutions. Chemically speaking, the BS(4,1) solution describes a high-spin Fe(II) ion ($S_{\text{Fe}} = 2$) coupled antiferromagnetically to a ligand radical ($S_L = 1/2$). The BS(3,0) solution could correspond either to an intermediate spin Fe(III) ($S_{\text{Fe}} = 3/2$) bound to a doubly reduced ligand ($S_L = 0$) or to a high-spin Fe(I) ($S_{\text{Fe}} = 3/2$) bound to a neutral ligand. Nevertheless, the BS(4,1) solution was found to be 10.7 kcal/mol lower in energy than the BS(3,0) state.

Table 4 presents selected bond lengths predicted by both calculations. Also included in Table 4 are the metrical parameters for **2-Cl**(Et_2O) (**2** = $(^{\text{Et}}\text{PDI})\text{Fe} = 2,6\text{-(2,6-Et}_2\text{C}_6\text{H}_3\text{N=CMe)}_2\text{C}_5\text{H}_3\text{N}$), the only known bis(imino)pyridine iron monochloride complex that has been structurally characterized.⁸ Despite diethyl ether coordination in the experimental structure, the calculated parameters from the BS(4,1) approach are in excellent agreement with the X-ray data. The metrical data from the favored broken symmetry calculation and the experimental data are in agreement with the monoreduced bis(imino)pyridine ligand, $[\text{PDI}]^-$, established from the reference compounds.

The zero-field Mössbauer spectrum of **1-Cl** recorded at 80 K (Figure 5) produced an isomer shift (δ) of 0.77 mm/s and a quadrupole splitting (ΔE_Q) = 0.73 mm/s, consistent with a high-spin iron(II) ion. The isomer shift is typical for four-coordinate ferrous ions and resembles that of the pseudo tetrahedral Fe(II)-S₄ sites in iron–sulfur clusters (δ = 0.7 mm/s).³⁴ For the BS(4,1) solution, the Mössbauer parameters for the truncated model

complex were computed as δ = 0.68 mm/s and ΔE_Q = 1.16 mm/s at 0 K. On the other hand, the BS(3,0) calculation yielded values of δ = 0.30 mm/s and ΔE_Q = −1.34 mm/s, further supporting the results from the BS(4,1) approach. While there is good agreement between the calculated and experimental isomer shifts, the disparity in the quadrupole splitting values may be a result of the truncated model used for the computational study.^{35,36} Similar effects have previously been observed for truncated models.^{35,36} However, due to the significant cost of calculating the full ligand system, we have not pursued this phenomenon further as we believe that it is of minor relevance to the conclusions that we have drawn.

Because the results of the BS(4,1) calculation successfully reproduced both experimental metrical parameters and the Mössbauer isomer shift, they provide a more accurate depiction of the electronic structure of **1-Cl** as compared to the BS(3,0) solution. A qualitative molecular orbital diagram computed from this solution for the truncated complex, $(^{\text{Me}}\text{pdi})\text{FeCl}$, is presented in Figure 6. There are four unpaired spin-up electrons in essentially metal-based orbitals, consistent with a high-spin iron(II) center. One of these orbitals, principally of d_z^2 parentage, interacts magnetically with a singly occupied (spin-down) b_2 orbital of the bis(imino)pyridine ligand. This interaction is antiferromagnetic with a large spatial overlap, S = 0.41, leading to a computed exchange coupling of J = −440 cm^{-1} . The Löwdin population analysis (Figure 6b)³⁷ is consistent with four unpaired electrons at the iron center and one unpaired electron on the bis(imino)pyridine ligand, delocalized over the conjugated π -system. Thus, the best electronic description for **1-Cl** is a high-spin iron(II) ion ($S_{\text{Fe}} = 2$) antiferromagnetically coupled to a ligand-centered radical ($S_L = 1/2$) delocalized on the bis(imino)pyridine chelate.

(ⁱPrPDI)FeL_n Compounds (L = CO, DMAP, N₂). The interesting catalytic activity of **1-(N₂)₂** prompted further investigation into the electronic structure of this and related compounds. As reported previously, **1-(N₂)₂** undergoes loss of dinitrogen in solution to furnish the four-coordinate mono(dinitrogen) complex, **1-N₂**. To avoid these complications, complexes were sought that did not undergo further chemistry in solution but had electronic properties similar to those of **1-(N₂)₂**. As reported previously,⁵ the bis(imino)pyridine iron dicarbonyl complex, **1-(CO)₂**, is a diamagnetic, thermally stable molecule. Unlike **1-(N₂)₂**, the ¹H and ¹³C NMR shifts in

(34) Beinert, H.; Holm, R. H.; Münck, E. *Science* **1997**, 277, 653.(35) Zhang, Y.; Mao, J.; Godbout, N.; Oldfield, E. *J. Am. Chem. Soc.* **2002**, 124, 13921.(36) Han, W.-G.; Liu, T.; Lovell, T.; Noodleman, L. *J. Am. Chem. Soc.* **2005**, 127, 15778.(37) Löwdin, P.-O. *Adv. Quantum Chem.* **1970**, 5, 185.

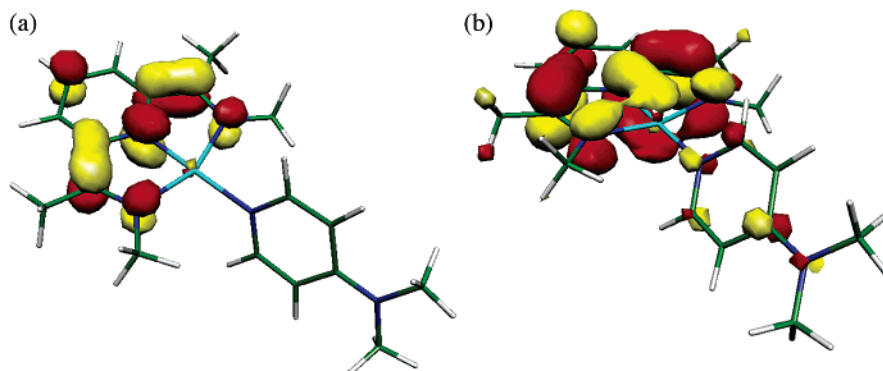


Figure 4. (a) Highest occupied SOMO of $[(\text{Me}_6\text{pdi})\text{Zn}(\text{DMAP})]^+$ from the DFT calculations. (b) DFT computed HOMO of $(\text{Me}_6\text{pdi})\text{Zn}(\text{DMAP})$.

Table 4. Selected Bond Distances (Å) and Angles (deg) Arising from Broken Symmetry DFT Calculations for $(\text{Me}_6\text{pdi})\text{FeCl}$ and Experimentally Determined Values for **2-Cl**(Et₂O)

	BS(4,1)	BS(3,1)	experimental
Fe(1)–N(1)	2.163	1.955	2.209(2)
Fe(1)–N(2)	2.028	1.882	2.009(2)
Fe(1)–N(3)	2.167	1.975	2.181(2)
Fe(1)–Cl(1)	2.253	2.037	2.2668(8)
N(1)–C(2)	1.311	1.340	1.301(3)
C(2)–C(3)	1.461	1.436	1.453(4)
C(3)–N(2)	1.371	1.375	
N(2)–C(7)	1.370	1.359	
C(7)–C(8)	1.461	1.438	1.443(3)
C(8)–N(3)	1.311	1.339	1.313(3)
N(1)–Fe(1)–N(3)	147	160	
N(2)–Fe(1)–Cl(1)	176	167	

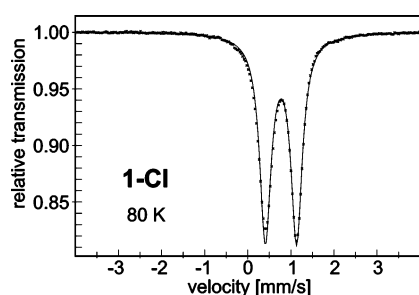


Figure 5. Zero-field Mössbauer spectrum of **1-Cl** recorded at 80 K.

benzene-*d*₆ are close to the diamagnetic reference values using the free bis(imino)pyridine ligand as the standard.

Although the NMR spectral properties of **1-(CO)₂** differ from those for the corresponding bis(dinitrogen) complex, the degree of bis(imino)pyridine ligand involvement was still of interest. Since our initial report,⁵ X-ray quality single crystals of **1-(CO)₂** were obtained from slow evaporation of THF from concentrated solutions over the course of 2 weeks. The solid-state structure of **1-(CO)₂** is presented in Figure 7 and, in analogy to **1-(N₂)₂**, exhibits an idealized square pyramidal iron center with apical and basal carbonyl ligands. The metrical parameters (Table 5) of the bis(imino)pyridine chelate are consistent with two electron reduction. Contracted C_{imine}–C_{ipso} distances of 1.425(2)/1.423(2) Å along with elongated N_{imine}–C_{imine} bond lengths of 1.330(2)/1.335(2) Å are comparable to the computed distances in **pdi-H₂** and $(\text{Me}_6\text{pdi})\text{Zn}(\text{DMAP})$.

To further investigate the electronic structure of **1-(CO)₂**, computational studies were conducted on the truncated model complex, (2,6-(C₆H₅N=CH)₂C₅H₃N)Fe(CO)₂ (**P^hpdi**)Fe(CO)₂ with both BS(1,1) and BS(0,0) strategies but led to the same

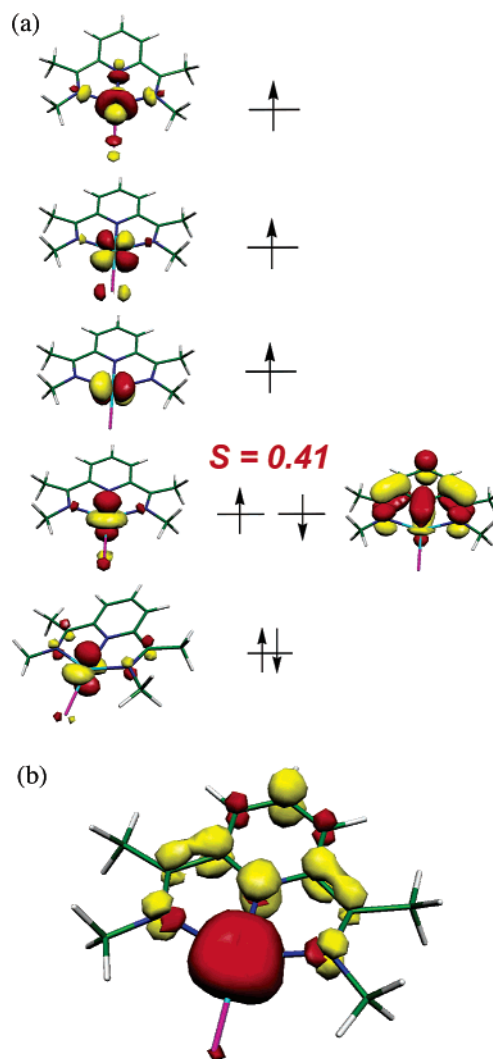


Figure 6. (a) Qualitative molecular orbital diagram for $(\text{Me}_6\text{pdi})\text{FeCl}$ computed from a B3LYP/TZVP BS(4,1) calculation; the singly occupied orbitals represent corresponding orbitals, whereas the doubly occupied orbital is a canonical orbital. (b) Total spin-density plot for $(\text{Me}_6\text{pdi})\text{FeCl}$ as derived from a broken symmetry (4,1) B3LYP/TZVP calculation. Positive spin-density is shown in red, and negative is shown in yellow.

BS(0,0) (e.g., closed-shell) solution. Because we have found a nontrivial complication in the analysis of the computational results, two different functionals (BP86, B3LYP) were used in this part of the study. The metrical data from these studies are presented along with the experimental data in Table 5. The two different functionals used produced similar bond distances that

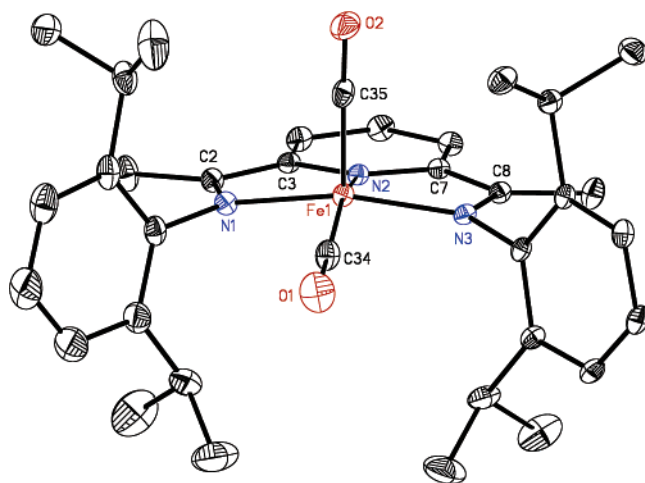


Figure 7. Molecular structure of **1-(CO)₂** at 30% probability ellipsoids. Hydrogen atoms are omitted for clarity.

Table 5. Selected Bond Distances (Å) for **1-(N₂)₂**, **1-(CO)₂** (Experimental), and **(^{Ph}pdi)Fe(CO)₂** Computed with the B3LYP and BP86 Functionals

	1-(N₂)₂^a	1-(CO)₂^b	(^{Ph}pdi)Fe(CO)₂	
			B3LYP	BP86
Fe(1)–N(a)	1.9452(16)	1.9622(15)	1.999	1.962
Fe(1)–N(b)	1.8362(14)	1.8488(14)	1.855	1.862
Fe(1)–N(c)	1.9473(16)	1.9500(14)	2.000	1.962
N(a)–C(2)	1.332(2)	1.330(2)	1.323	1.338
C(2)–C(3)	1.428(3)	1.425(2)	1.413	1.415
C(3)–N(b)	1.379(2)	1.376(2)	1.377	1.384
N(b)–C(7)	1.376(2)	1.372(2)	1.377	1.384
C(7)–C(8)	1.427(2)	1.423(2)	1.413	1.415
C(8)–N(c)	1.333(2)	1.335(2)	1.323	1.338

^a N(a) = N(5), N(b) = N(6), N(c) = N(7). ^b N(a) = N(1), N(b) = N(2), N(c) = N(3).

are in good agreement with the experimentally determined structure with slightly more accurate values being observed for the BP86 method. Notably, the contracted C_{imine}–C_{ipso} and elongated N_{imine}–C_{imine} distances are consistent with a [PDI]^{2–} ligand. The quality of the computational results is also highlighted by the agreement of the calculated and experimental infrared carbonyl stretching frequencies. The BP86 calculations yielded values of 1929 and 1978 cm^{–1} for (^{Ph}pdi)Fe(CO)₂, which are in good agreement with the experimentally determined frequencies of 1914 and 1974 cm^{–1} for **1-(CO)₂**.

The zero-field Mössbauer spectrum of **1-(CO)₂** was recorded at 80 K (Figure S2) and produced an isomer shift of 0.03 mm/s and a quadrupole splitting of 1.17 mm/s. These values were reproduced by the 0 K computation on the model complex, (^{Ph}pdi)Fe(CO)₂. The B3LYP functional yielded values of δ = 0.05 mm/s and ΔE_Q = 1.38 mm/s, while the BP86 functional produced nearly identical values (δ = 0.02 mm/s; ΔE_Q = 1.15 mm/s).

A molecular orbital diagram obtained from the optimized structure of (^{Ph}pdi)Fe(CO)₂ using the BP86 functional is presented in Figure 8. Analogous results were obtained for the B3LYP functional. The *z* axis was defined along the normal of the complex and *y* axis along the C₂ axis containing the Fe–N_{pyridine} bond. Three principally metal-based orbitals, d_{xy}, d_{xz}, and an admixture of d_{yz/z²}, are doubly occupied and are involved in back-donation to the two carbonyl ligands. Notably, the HOMO contains 68% bis(imino)pyridine ligand character that resembles the b₂ molecular orbital computed for pdi-H₂. In this

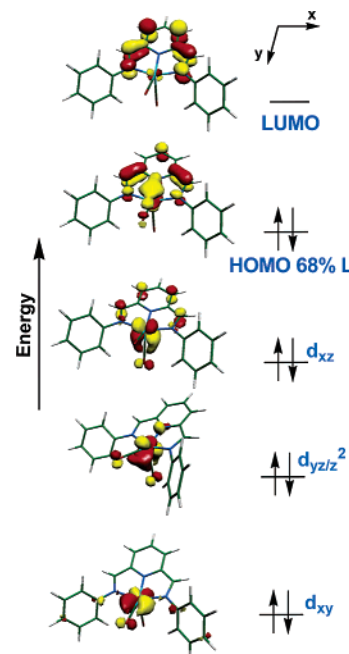
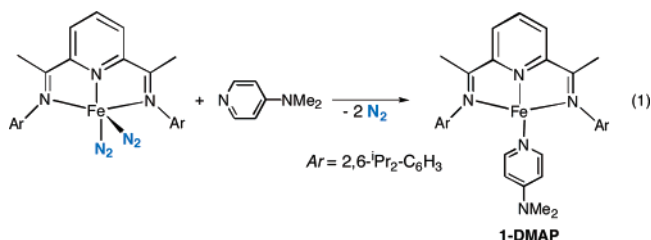


Figure 8. Partial molecular orbital diagram for (^{Ph}pdi)Fe(CO)₂ determined from the BP86/TZVP calculation with unoccupied d_{x²–y²} (LUMO+1) and d_{x²–y²} (LUMO+2) omitted.

limit and in combination with the metrical parameters, the iron can be formulated as low-spin Fe(II) complexed with a dianionic bis(imino)pyridine ligand, [PDI]^{2–}. However, there is significant contribution in the HOMO from iron orbitals, and in combination with the Mössbauer parameters this suggests that an iron(0), d⁸ formulation may also be acceptable as originally proposed.⁵

With a description of the electronic structure of a “purely” diamagnetic compound in hand, spectroscopic and computational studies of molecules that exhibit unusual NMR features were performed. For these reasons, a thermally stable bis(imino)pyridine iron derivative was targeted that displayed the unusual NMR chemical shifts of **1-(N₂)₂** but was not complicated by competing ligand dissociation processes. Treatment of **1-(N₂)₂** with 1 equiv of a principally σ -donating ligand such as 4-(*N,N*-dimethylamino)pyridine (DMAP) yielded a purple solid identified as the four-coordinate compound, **1-DMAP** (eq 1).



The ¹H NMR spectrum of **1-DMAP** (Figure 9) exhibits features reminiscent of **1-(N₂)₂/1-N₂**.⁵ The hydrogens orthogonal to the iron–bis(imino)pyridine chelate plane (e.g., those on the isopropyl aryl substituents) are close to the diamagnetic reference values for the free ligand and diamagnetic **1-(CO)₂**,⁵ while those in the plane of the iron are shifted. Notably, the singlet for the imine methyl hydrogens shifts upfield from 2.08 ppm in **1-(CO)₂** to –5.58 ppm in **1-DMAP**. Likewise, the *m*-pyridine shifts downfield to 12.42 ppm in **1-DMAP** from 7.63 ppm in **1-(CO)₂**. Despite the increase in chemical shift dispersion in

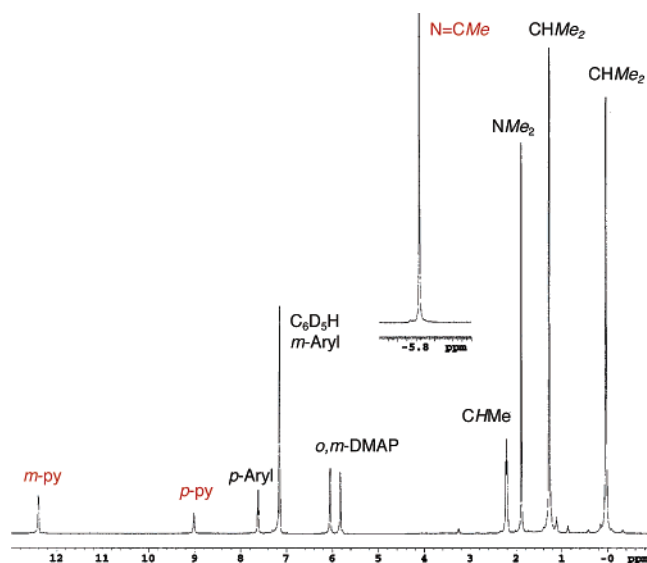


Figure 9. ^1H NMR spectrum of **1-DMAP** at 23 °C in benzene- d_6 .

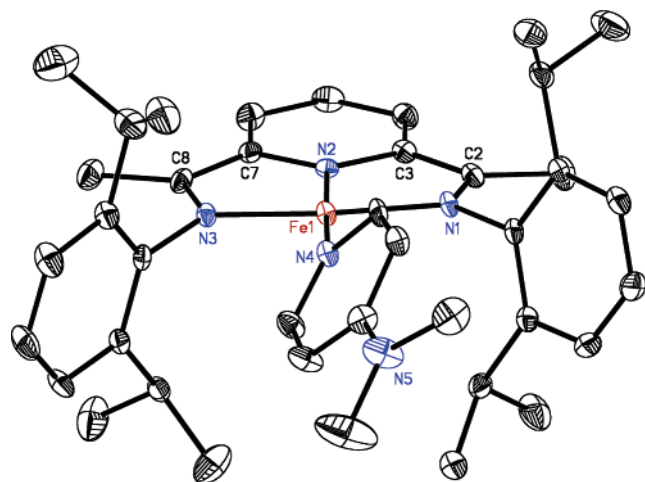


Figure 10. Molecular structure of **1-DMAP** at 30% probability ellipsoids. Hydrogen atoms are omitted for clarity.

compounds such as **1-DMAP** and **1-(N₂)₂/1-N₂**, these values are approximately 10-fold less than typical paramagnetic shifts in compounds such as **1-Cl₂**³ and **1-Cl**.⁸ This behavior suggests that **1-DMAP** is actually diamagnetic and the unusual shifts of the in-plane hydrogens on the chelate are a result of temperature-independent paramagnetism (TIP) whereby an excited state mixes into the singlet ground state. Similar behavior has been observed by Budzelaar and co-workers in the related cobalt(I) compounds, (PDI)CoX (X = alkyl, halide).³⁸ For **1-DMAP**, the resonances for the DMAP heterocycle are close to their diamagnetic reference values and demonstrate that the π -system is not in conjugation with the metal center (vide infra).

Single crystals of **1-DMAP** were grown from a concentrated pentane–ether solution cooled to -35 °C. The solid-state structure (Figure 10) confirms a four-coordinate, square planar compound with the DMAP ligand tilted 46.2° from the iron–bis(imino)pyridine chelate plane. While the metrical parameters (Table 6) will be discussed in more detail with the computational results, they are clearly indicative of a doubly reduced bis(imino)pyridine dianion, [PDI]²⁻.

Table 6. Energies, Mössbauer Parameters, and Selected Bond Distances (Å) and Angles (deg) for **1-DMAP** and Various Computational Models

	1-DMAP (exp)	BS(2,2)	BS(3,1)	BS(4,2)	BS(0,0)
relative energy (kcal/mol)		0.0	2.5	6.5	23
δ (mm/s)	0.31	0.29	0.32	0.64	0.25
ΔE_Q	1.94	−0.82	1.07	−0.97	−1.67
η	0.40	0.46	0.73	0.55	0.59
Fe(1)–N(1)	1.908(3)	1.949	1.968	2.042	1.939
Fe(1)–N(2)	1.821(3)	1.869	1.837	2.020	1.800
Fe(1)–N(3)	1.943(3)	1.950	1.988	2.041	1.939
Fe(1)–N(4)	1.979(3)	2.030	2.039	2.157	2.025
N(1)–C(2)	1.350(5)	1.365	1.361	1.359	1.342
C(2)–C(3)	1.414(5)	1.427	1.418	1.439	1.429
C(3)–N(2)	1.390(5)	1.373	1.386	1.364	1.393
N(2)–C(7)	1.387(5)	1.373	1.390	1.363	1.393
C(7)–C(8)	1.406(5)	1.427	1.426	1.439	1.429
C(8)–N(3)	1.358(5)	1.365	1.363	1.359	1.342
N(1)–Fe(1)–N(3)	161.38(14)	164	163	153	163
N(2)–Fe(1)–N(4)	175.58(14)	180	180	144	180

Confirmation of the diamagnetic ground state of **1-DMAP** has been provided by solution (Evans method) and solid-state magnetometry (SQUID, magnetic susceptibility balance). Extreme care must be taken when making these measurements, as **1-DMAP** is a sensitive compound. Over the course of days in either the solid state or solution, the magnetic moments of samples of **1-DMAP** steadily increase. Significantly, no change in the ^1H NMR chemical shifts or Mössbauer spectra was observed on fresh (diamagnetic) or aged material (paramagnetic). However, monitoring benzene- d_6 solutions of the compound over the course of days at 23 °C and integrating the resonances versus an internal standard (ferrocene, benzene) revealed gradual disappearance of the peaks for **1-DMAP**. Importantly, no new peaks (free $^i\text{PrPDI}$, free DMAP from exposure to air or water) were observed. Therefore, the only evidence of the chemical change for **1-DMAP** over time is the decrease in the intensity of the resonances in the ^1H NMR spectrum and increase in magnetic moment. The origin of this behavior and the identity of the compound that results from this transformation remain unknown.

To gain further insight into the origin of the unusual ^1H NMR shifts and to assign the oxidation state of both the ligand and the metal in **1-DMAP**, the electronic structure of the molecule was investigated computationally using the model complex, ($^{\text{Me}}\text{pdi})\text{Fe}(\text{DMAP})$. Five different coupling schemes, two diamagnetic ($S = 0$) and three paramagnetic ($S = 1$), were examined using the B3LYP functional. The closed-shell configurations were BS(0,0) and BS(2,2), while the open-shell cases were BS(3,1) and BS(4,2). A fifth possibility, BS(2,0), was also considered and converged to the same solution as BS(3,1), and the two will no longer be distinguished. The relative energies, computed and experimental metrical data, and Mössbauer parameters are compiled in Table 6. The lowest energy was found for the BS(2,2) solution, only 2.5 kcal/mol below the BS(3,1) state. Given the use of model compounds and the error bars associated with the calculations, these states are essentially isoenergetic. The BS(4,2) and BS(0,0) solutions are higher in energy than the ground state by 6.5 and 23 kcal/mol, respectively.

Comparison of the metrical data from the crystal structure of **1-DMAP** to the bond distances and angles obtained from

(38) Knijnenburg, Q.; Hetterscheid, D.; Kooistra, T. M.; Budzelaar, P. H. M. *Eur. J. Inorg. Chem.* **2004**, 1204.

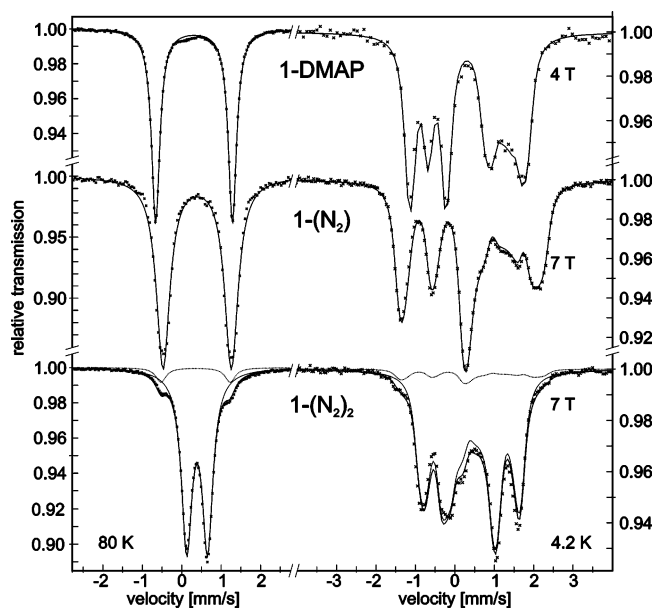


Figure 11. Mössbauer spectra of **1-DMAP**, **1-(N₂)**, and **1-(N₂)₂** recorded at 80 K in zero-field (left column) and at 4.2 K with applied fields as indicated (right column). The lines are fits with Lorentzian doublets for the zero-field spectra and magnetic simulations for $S = 0$ with the usual nuclear Hamiltonian for the magnetic spectra. The Mössbauer parameters are given in the text or in Table 6. The dotted lines in the spectra from **1-(N₂)₂** represent a 7.5% contamination with **1-(N₂)**.

the BS(2,2) and BS(3,1) optimized structures of the model compound (Table 6) reveals good agreement between theory and experiment. The average Fe–N_{imine} and Fe–N_{pyridine} distances are slightly overestimated as is typical for the B3LYP functional,^{30c,d} while the bond lengths for the bis(imino)pyridine ligand are well reproduced by both the BS(2,2) and the BS(3,1) solutions. By way of comparison, the BS(4,2) results significantly overestimate the iron–nitrogen bond distances and underestimate the N(2)–Fe(1)–N(3) bond angle by 30°. Importantly, the computed BS(2,2) and the BS(3,1) parameters and experimental bond distances are indicative of the doubly reduced bis(imino)pyridine dianion, [PDI]^{2−}.²¹

The zero-field Mössbauer spectrum of **1-DMAP** was recorded at 80 K (Figure 11) and produced an isomer shift of 0.31 mm/s and quadrupole splitting of +1.94 mm/s, consistent with an intermediate spin ($S_{\text{Fe}} = 1$) Fe(II), d⁶ ion.³⁹ Measurements made at 4.2 K with applied fields in the range of $B = 1$ –7 T exhibit the typical magnetic splitting pattern according to the external field. Importantly, there is no indication of the presence of significant internal fields. The simulation of the $B = 7$ T spectrum (Figure 11, top right) with a total spin of $S = 0$ is in accord with the diamagnetic ground state of the molecule. The applied-field Mössbauer spectrum also established a positive sign of the quadrupole splitting and an asymmetry parameter for the electric field gradient (efg) of $\eta = 0.40(5)$.

The isomer shifts of 0.29 and 0.32 mm/s computed for the BS(2,2) and BS(3,1) states on the truncated model complex, (^Mpdi)Fe(DMAP), are in excellent agreement with the experimental value and further support the oxidation state assignment of the iron as ferrous. However, the computed quadrupole splitting values are predicted as −0.82 and +1.07 mm/s for the

diamagnetic BS(2,2) and paramagnetic BS(3,1) states, respectively. Both values disagree with the experimental findings. Recall **1-DMAP** is diamagnetic and possesses a positive sign for the quadrupole moment. Because the experimental isomer shifts have been reproduced by the calculations, the discrepancy between the computed and measured quadrupole splittings is not explained presently. Nevertheless, we have frequently observed a high-sensitivity of the computed quadrupole splittings to details of the molecular model, in particular to truncation effects of the ligands. However, the computed isomer shifts are much less sensitive to such details of the calculations that are of very limited importance for the overall electronic structure. We therefore feel that the computed isomer shifts provide sufficient evidence for reasonable electronic structures. Importantly, the δ values of 0.64 and 0.25 mm/s from the BS(4,2) and BS(0,0) calculations do not agree with the experimental isomer shifts (Table 6), further suggesting these states do not accurately model the electronic structure of **1-DMAP**.

Qualitative molecular orbital diagrams computed from the BS(2,2) and BS(3,1) approaches for (^Mpdi)Fe(DMAP) are presented in Figure 12. The z axis was chosen as the normal of the complex, and the x axis lies on the iron–imine bonds. Qualitatively the two states are similar with intermediate spin ($S_{\text{Fe}} = 1$) ferrous ions. The difference is in the spin state of bis(imino)pyridine dianions. In the BS(2,2) case, the metal is antiferromagnetically coupled to a triplet ($S_{\text{L}} = 1$) bis(imino)pyridine dianion to yield an overall $S = 0$ spin state. The d_{yz} and d_{xz} iron orbitals interact strongly ($J = -900 \text{ cm}^{-1}$) with the b_2 and a_2 ligand orbitals, respectively. The adiabatically computed excited quintet state is 11 kcal/mol higher in energy. For the BS(3,1) structure, the two unpaired electrons are iron-based and principally of d_{xz} and d_{yz} parentage. The bis(imino)pyridine ligand is in a singlet ground state ($S_{\text{L}} = 0$), a result of a set of orbitals in the spin-up and spin-down manifold that resemble b_2 of **pdi-H₂**. These orbitals exhibit spin coupling via a π -pathway with a large mutual spatial overlap of $S = 0.76$, resulting in strong antiferromagnetic coupling. Consistent with this view is the calculation of a relatively large exchange-coupling constant of $J = -950 \text{ cm}^{-1}$. Thus, the two nearly isoenergetic solutions represent spin crossover in the bis(imino)pyridine ligand, where both spin singlet ($S_{\text{L}} = 0$) and triplet ($S_{\text{L}} = 1$) states are close in energy. These results are similar to those obtained for free **pdi-H₂** where the triplet was calculated (4.3 kcal/mol, ab initio; 2.3 kcal/mol, DFT) to be slightly lower in energy than the singlet.

In the BS(3,1) solution, the computational and experimental data support an intermediate spin ferrous ion that is coordinated to a singlet diradical ($S_{\text{L}} = 0$) bis(imino)pyridine dianion, [PDI]^{2−}. The singlet state arises from antiferromagnetic coupling through an iron orbital in agreement with the Goodenough–Kanamori rules.⁴⁰ Analysis of the total spin population (Figure S3) reveals positive spin-density at the iron center and one C_{ipso}–C_{imine}–N_{imine} unit corresponding to three unpaired electrons, with two localized at the metal. The second C_{ipso}–C_{imine}–N_{imine} unit carries a spin population of about one-electron but of opposite sign. It should be noted that the occurrence of net spin-density within the singlet diradical unit is an artifact of the broken symmetry method in the sense that the singlet-

(39) (a) Dale, B. W.; Williams, R. J.; Edwards, P. R.; Johnson, C. E. *J. Chem. Phys.* **1968**, *49*, 3445. (b) Ray, K.; Begum, A.; Weyermüller, T.; Piligkos, S.; van Slageren, J.; Neese, F.; Wieghardt, K. *J. Am. Chem. Soc.* **2005**, *127*, 4403. (c) Hawrelak, E. J.; Bernskoetter, W. H.; Lobkovsky, E.; Yee, G. T.; Bill, E.; Chirik, P. J. *Inorg. Chem.* **2005**, *44*, 3103.

(40) (a) Kahn, O. *Molecular Magnetism*; Wiley–VCH: New York, 1993. (b) Kanamori, J. *J. Phys. Chem. Solids* **1959**, *10*, 87. (c) Goodenough, J. B. *J. Phys. Chem. Solids* **1958**, *6*, 287. (d) Goodenough, J. B. *Phys. Rev.* **1955**, *100*, 564.

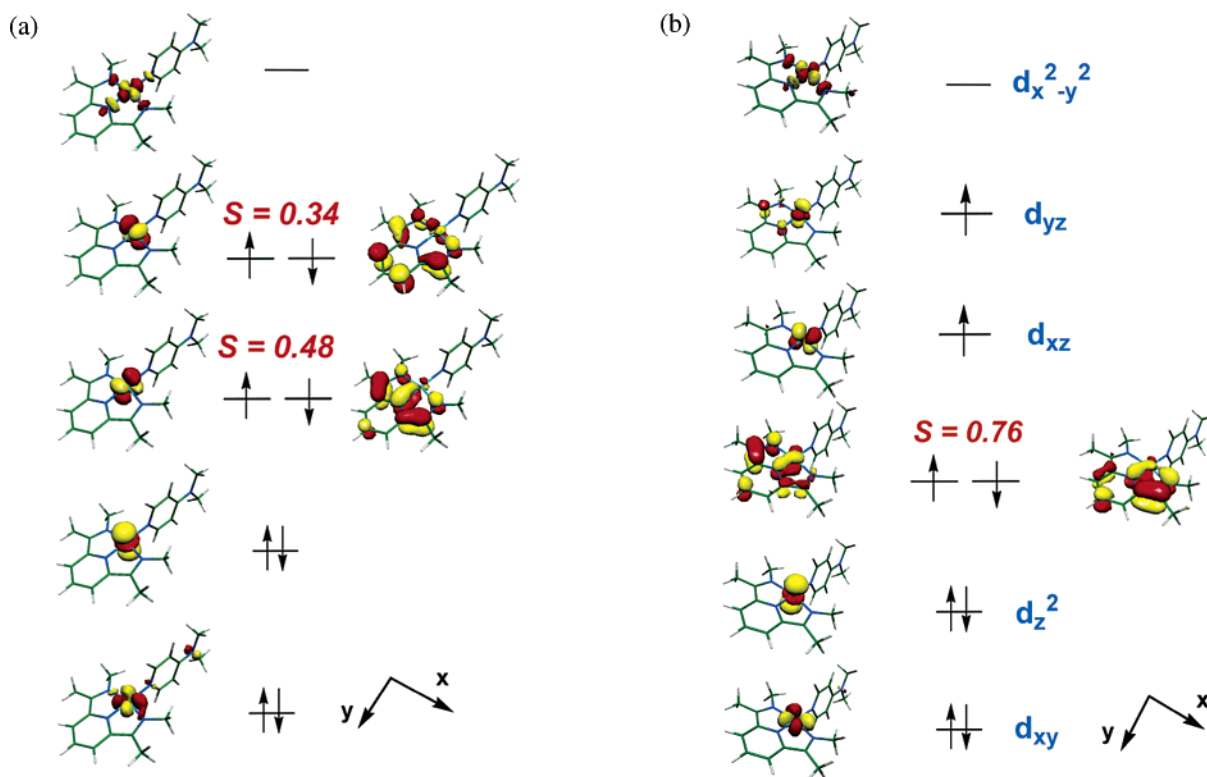


Figure 12. Qualitative molecular orbital diagram for $(\text{MePDI})\text{Fe}(\text{DMAP})$ derived from BS(2,2) (left) and BS(3,1) (right) B3LYP/TZVP calculations; the singly occupied orbitals represent corresponding orbitals, whereas the doubly occupied and unoccupied orbitals are canonical orbitals.

coupled pair does not contribute to any spin-density in reality. The broken symmetry spin densities are nevertheless highly suggestive as they indicate the distribution of the unpaired electrons concisely. It is also worth noting that the higher energy BS(4,2) structure corresponds to a high-spin iron(II) compound coupled to a triplet diradical ($S_L = 1$) $[\text{PDI}]^{2-}$ ligand (Figure S4).

The combined results of the computational, spectroscopic, and structural study of **1-DMAP** clearly establish the oxidation state of iron and the bis(imino)pyridine and also account for the unusual ^1H NMR shifts. The data support an intermediate spin ferrous ion complexed by a bis(imino)pyridine dianion, $[\text{PDI}]^{2-}$. The $[\text{PDI}]^{2-}$ has two nearly isoenergetic spin states with the triplet ($S_L = 1$) computed slightly lower than the singlet ($S_L = 0$). As a result, the ground state of **1-DMAP** is diamagnetic and is described by the BS(2,2) solution where the ferrous ion ($S_L = 1$) is antiferromagnetically coupled to the triplet ($S_L = 1$) bis(imino)pyridine dianion. Importantly, the triplet excited state, as described by the BS(3,1) model, where the only difference is the singlet spin state of the chelate ($S_L = 0$) giving rise to an overall $S = 1$ configuration, is energetically accessible and mixes into the ground state most likely via spin-orbital coupling. We note, however, that thermal population of excited paramagnetic states was not observed from the magnetic measurements. Thus, the unusual chemical shifts observed for the in-plane hydrogens are a result of temperature-independent paramagnetism rather than from Curie–Weiss behavior.³⁸ Notably, the peaks that exhibit the largest shifts, the imine methyl groups and the *m*-pyridine, have the largest coefficients and hence electron density as computed in the BS(3,1) state (Figure 10).

To further experimentally probe this model, the variable-temperature ^1H NMR spectra of **1-DMAP** were recorded in

toluene- d_8 . If the anomalous chemical shifts were a result of Curie behavior (or paramagnetic impurities), the δ values would be expected to change dramatically as a function of temperature. If the proposed TIP phenomenon is operative, then the chemical shifts should not change as a function of temperature. As presented in Figure 13, the peaks for both the imine methyl groups and the *m*-pyridine do not shift over an approximately 100 °C temperature range (−80 to 23 °C). The observation of ^{13}C resonances close to those observed in the free ligand and **1-(CO)₂** also supports a diamagnetic ground state with a TIP contribution rather than a true Curie–Weiss paramagnet.

Having established definitive spectroscopic and metrical parameters for bis(imino)pyridine ligand involvement, the electronic structure of the catalytic precursor, **1-(N₂)₂**, was reevaluated. The bond length data (Table 5)⁵ from the solid-state structure are comparable to **1-(CO)₂** and support two electron reduction of the chelate to form an $[\text{PDI}]^{2-}$ ligand. The $\text{N}_{\text{imine}}-\text{C}_{\text{imine}}$ distances are elongated to 1.332(2) and 1.333(2) Å, while the $\text{C}_{\text{imine}}-\text{C}_{\text{ipso}}$ values are contracted to 1.428(3) and 1.427(2) Å. These distortions are slightly less pronounced than in **1-DMAP** and are most likely a consequence of the π -accepting (albeit weak) ability of the N_2 ligands as compared to the σ -only heterocycle.

The zero-field Mössbauer spectrum of **1-(N₂)₂** was recorded at 80 K and is presented in Figure 11 (bottom). The experimentally determined isomer shift of 0.39 mm/s and a quadrupole splitting of 0.53 mm/s are consistent with intermediate spin iron(II). The spectrum also contains 7.5% of another iron compound, subsequently identified as the monodinitrogen complex, **1-(N₂)**, arising from N_2 dissociation from **1-(N₂)₂**. The Mössbauer data for pure samples of **1-(N₂)** produced a $\delta = 0.38$ mm/s with $\Delta E_Q = 1.72$ mm/s, consistent with an electronic structure for the iron similar to that in **1-(N₂)₂**.

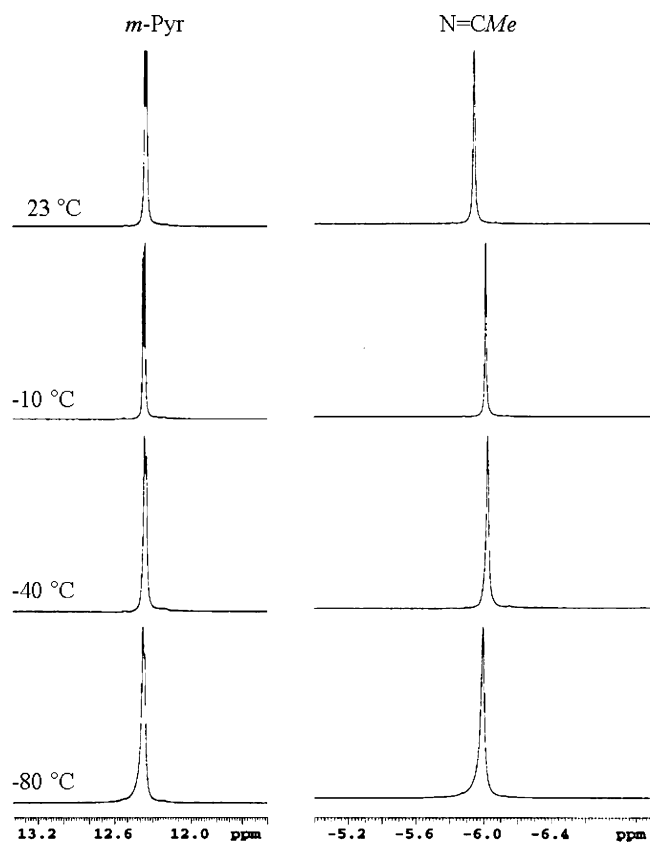


Figure 13. Partial ^1H NMR spectra of **1-DMAP** as a function of temperature in toluene- d_8 .

Applied-field spectra of **1-(N₂)** and **1-(N₂)₂** reveal diamagnetic ground states for both compounds, as observed above for **1-DMAP**. The magnetic spectra shown in Figure 11, right middle and bottom, were recorded at 4.2 K with 7 T field and could be readily simulated by assuming $S = 0$. The parameters obtained for the electric field gradients, however, show in detail some difference in the electronic structures of **1-DMAP**, **1-(N₂)**, and **1-(N₂)₂**. The sign of the quadrupole splitting is found to be positive for **1-(N₂)** with the asymmetry parameter $\eta = 0.4$, which is very close to the values for **1-DMAP** ($\Delta E_Q = +1.94$ mm/s, $\eta = 0.4$), whereas ΔE_Q is negative for **1-(N₂)₂** with $\eta = 0.6$. We explain this difference by the different coordination symmetries of the compounds. The intermediate spin state of iron(II) in both planar compounds, **1-DMAP** and **1-(N₂)**, results from the classical “one-over-four” ligand field splitting of d-orbitals for planar four-coordination, which is usually accompanied by large positive electric field gradients. Apparently, the structure of the dinitrogen compound **1-(N₂)₂** deviates

considerably from this pattern and shows ferrous-intermediate spin for a very asymmetric five-coordination of iron.

The combined spectroscopic and structural data strongly support an intermediate ferrous ion coordinated by a bis(imino)pyridine dianion, $[\text{PDI}]^{2-}$, in both **1-(N₂)₂** and **1-N₂**. This view of the electronic structure is corroborated by the pentane solution infrared spectroscopic data in our initial report,⁵ where the N≡N stretches of 2073 and 2132 cm^{-1} for **1-(N₂)₂** indicate little π -back-bonding from the iron to the N₂ ligands and are most consistent with iron(II) rather than iron(0). A similar high-frequency N₂ stretch centered at 2046 cm^{-1} was observed for **1-(N₂)**, again consistent with a ferrous ion in the four-coordinate compound.

Concluding Remarks

The combined spectroscopic, structural, and computational studies have resulted in a comprehensive picture of the electronic structure of a family of bis(imino)pyridine iron compounds. As summarized in Figure 14, single electron reduction of **1-Cl₂** to furnish **1-Cl** occurs with formal reduction of the bis(imino)pyridine ligand, not the iron center. Similar behavior has been observed in related cobalt chemistry.³⁸ The metrical data, Mössbauer parameters, and computational results support high-spin, $S = 2$ ferrous ions in both complexes. In the latter, addition of an electron to the complex resulted in a bis(imino)pyridine ligand-centered radical ($S_L = 1/2$) antiferromagnetically coupled to the iron center ($S_{\text{Fe}} = 2$) to account for the overall $S = 3/2$ ground state.

Subsequent one electron reduction of **1-Cl** in the presence of weak field ligands such as DMAP or dinitrogen again results in reduction of the bis(imino)pyridine chelate, furnishing a dianionic $[\text{PDI}]^{2-}$ fragment complexed to an intermediate spin ferrous ion. For the DMAP case, mixing of an overall $S = 1$ excited state into the $S = 0$ ground state by spin-orbital coupling results in temperature-independent paramagnetism that shifts the in-plane hydrogens in the solution NMR spectra. The computational studies also demonstrate that the singlet diradical bis(imino)pyridine ligands in the excited states arise from superexchange through a doubly occupied iron orbital in agreement with the Goodenough–Kanamori rules. Coordination of this type is another example of the “excited-state coordination” concept previously described.²⁴

One electron reduction of **1-Cl** in the presence of a strong field ligand such as carbon monoxide produced a diamagnetic compound where again the bis(imino)pyridine exhibits metrical parameters consistent with two electron reduction and hence an iron(II) center. However, in this case, significant contributions from iron(0)-like resonance structures cannot be excluded. Taken

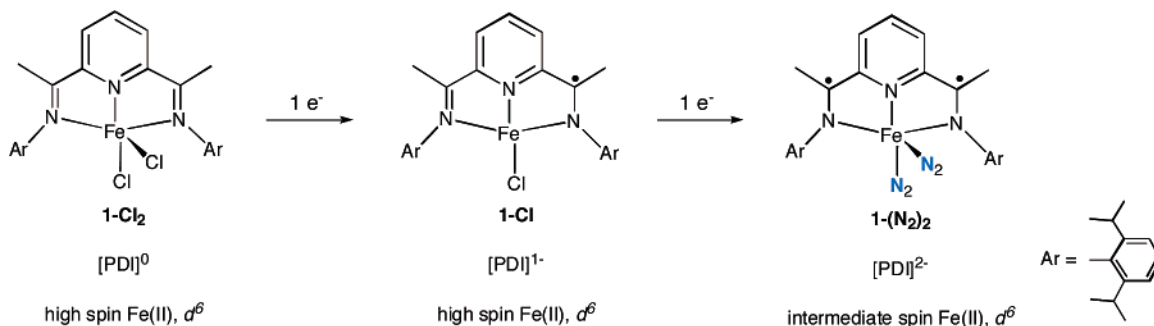


Figure 14. Summary of the electronic structure of bis(imino)pyridine iron compounds.

together, the results presented herein provide a systematic classification of experimental and computational parameters for the degree of reduction of bis(imino)pyridine ligands in iron chemistry. Given the importance of these molecules in supporting catalytically active iron compounds, these parameters may prove important in understanding the mechanisms of various bond-forming reactions.

Experimental Section

General Considerations. All air- and moisture-sensitive manipulations were carried out using standard vacuum line, Schlenk, and cannula techniques or in an MBraun inert atmosphere drybox containing an atmosphere of purified nitrogen. The drybox was equipped with a cold well designed for freezing samples in liquid nitrogen. Solvents for air- and moisture-sensitive manipulations were initially dried and deoxygenated using literature procedures.⁴¹ Argon and hydrogen gas were purchased from Airgas Inc. and passed through a column containing manganese oxide supported on vermiculite and 4 Å molecular sieves before admission to the high vacuum line. Benzene-*d*₆ was purchased from Cambridge Isotope Laboratories and distilled from sodium metal under an atmosphere of argon and stored over 4 Å molecular sieves and sodium metal. **1-Cl**, **1-(N₂)₂**, and **1-(CO)₂** were prepared according to literature procedures.^{5,8} 4-(*N,N*-Dimethylamino)pyridine was purchased from Acros and sublimed before use.

¹H NMR spectra were recorded on Varian Mercury 300 and Inova 400 and 500 spectrometers operating at 299.763, 399.780, and 500.62 MHz, respectively. All chemical shifts are reported relative to SiMe₄ using ¹H (residual) chemical shifts of the solvent as a secondary standard. Solution magnetic moments were determined by the Evans method⁴² using a ferrocene standard and are the average value of at least two independent measurements, unless stated otherwise. Elemental analyses were performed at Robertson Microlit Laboratories, Inc., in Madison, NJ.

Single crystals suitable for X-ray diffraction were coated with polyisobutylene oil in a drybox, transferred to a nylon loop, and then quickly transferred to the goniometer head of a Bruker X8 APEX2 diffractometer equipped with a molybdenum X-ray tube ($\lambda = 0.71073$ Å). Preliminary data revealed the crystal system. A hemisphere routine was used for data collection and determination of lattice constants. The space group was identified and the data were processed using the Bruker SAINT+ program and corrected for absorption using SADABS. The structures were solved using direct methods (SHELXS) completed by subsequent Fourier synthesis and refined by full-matrix least-squares procedures.

Mössbauer data were collected on an alternating constant-acceleration spectrometer. The minimum experimental line width was 0.24 mm s⁻¹ (full width at half-height). A constant sample temperature was maintained with an Oxford Instruments Variox or an Oxford Instruments Mössbauer-Spectromag 2000 cryostat. Reported isomer shifts (δ) are referenced to iron metal at 293 K.

Computational Methods. All DFT and ab initio calculations were performed with the ORCA program package.⁴³ The geometry optimizations of complexes were carried out at either the B3LYP^{44,45} or the BP86 level^{44,46} of DFT. The all-electron Gaussian basis sets were those developed by the Ahlrichs group.⁴⁷ For **1-DMAP** and **1-Cl** calculations,

the two 2,6-diisopropylphenyl groups of the pyridine(diimine) ligand (abbreviated to PDI) were substituted by two CH₃ units. For **1-(CO)₂**, the four isopropyl groups of the two phenyl rings and two methyl groups of the PDI ligand were replaced by six hydrogen atoms.

Studies of free unsubstituted ligands were performed with the CASSCF/IDDCI3 methods.²⁸ Initially, the geometry was optimized using BP86 DFT with a TZVP basis set. For the CASSCF study at the BP86 geometry, the structure was doubly protonated at the imino-nitrogen atoms to compensate for the overall negative charge of the molecule. The structure was reoptimized at the CASSCF(2,2) level with the SV(P) basis set and compared to an RHF optimized structure of the neutral (unprotonated) compound.

Corresponding,²⁹ canonical, and quasirestricted⁴⁸ orbitals and density plots were obtained by the program Molekel.⁴⁹ IR spectra of **1-(CO)₂** were calculated with the BP86 functional on the optimized geometries using two-sided numerical finite differences of analytical gradients. Nonrelativistic single point calculations on the optimized geometries of iron complexes with the B3LYP functional were carried out to predict Mössbauer spectral parameters (isomer shifts and quadrupole splittings). These calculations employed the CP(PPP) basis set²⁵ for iron and the TZVP basis sets for N, C, O, and Cl atoms. The Mössbauer isomer shifts were calculated from the computed electron densities at the iron centers as previously described.⁵⁰

Preparation of (PrPDI)Fe(DMAP) (1-DMAP). A 20 mL scintillation vial was charged with 0.052 g (0.088 mmol) of **1-(N₂)₂** and approximately 10 mL of diethyl ether. With stirring, 0.011 g (0.088 mmol) of 4-(*N,N*-dimethylamino)pyridine was added, resulting in an immediate color change from olive green to reddish-purple. The resulting reaction mixture was stirred for 10 min, after which time the volatiles were removed in vacuo to yield 0.056 g (98%) of a red-purple solid identified as **1-DMAP**. Washing the solid on a fritted funnel with dry pentane produced spectroscopically and magnetically pure compound. Anal. Calcd for C₄₀H₅₃N₅Fe: C, 72.82; H, 8.10; N, 10.62. Found: C, 72.60; H, 8.00; N, 10.45. ¹H NMR (benzene-*d*₆): $\delta = -5.85$ (s, 6H, C(*Me*)), 0.07 (d, 6.63 Hz, 12H, CHMe₂), 1.29 (d, 5.80 Hz, 12H, CHMe₂), 1.91 (s, 6H, N(CH₃)₂), 2.24 (sept, 6.63 Hz, 4H, CHMe₂), 5.84 (d, 6.84 Hz, 2H, *o*- or *m*-DMAP), 6.07 (d, 6.84 Hz, 2H, *o*- or *m*-DMAP), 7.17 (m, 2H, *p*-aryl), 7.64 (dd, 7.85 Hz, 4H, *m*-aryl), 9.04 (t, 8.50 Hz, 1H, *p*-pyridine), 12.42 (d, 8.50 Hz, 2H, *m*-pyridine). ¹³C NMR (benzene-*d*₆): $\delta = 23.16$ (CHMe₂), 24.53 (CHMe₂), 29.00 (CHMe₂), 38.28 (C(*Me*) and NMe₂), 102.90 (*m*-pyridine or *p*-aryl), 107.51 (*m*- or *o*-DMAP), 123.88 (*m*-aryl), 124.44 (*m*-pyridine or *p*-aryl), 136.73, 141.52 (*p*-pyridine), 151.40 (*m*- or *o*-DMAP), 165.66, 166.52, 190.44.

Acknowledgment. The Cornell group thanks the David and Lucile Packard Foundation for financial support. P.J.C. is a Cottrell Scholar of the Research Corporation and a Camille Dreyfus Teacher-Scholar. The Mülheim group thanks the Max-Planck-Society and the Fond der Chemischen Industrie for financial support of this work.

Supporting Information Available: Additional spectroscopic data, computational results, and structural data for **1-(CO)₂** and **1-DMAP**. This material is available free of charge via the Internet at <http://pubs.acs.org>.

JA064557B

- (41) Pangborn, A. B.; Giardello, M. A.; Grubbs, R. H.; Rosen, R. K.; Timmers, F. J. *Organometallics* **1996**, *15*, 1518.
(42) Sur, S. K. *J. Magn. Reson.* **1989**, *82*, 169.
(43) Neese, F. *ORCA, an Ab Initio, Density Functional and Semiempirical Electronic Structure Program Package*, version 2.4, revision 36; Max-Planck Institut für Bioanorganische Chemie: Mülheim/Ruhr, Germany, May 2005.
(44) Becke, A. D. *J. Chem. Phys.* **1986**, *84*, 4524.
(45) (a) Becke, A. D. *J. Chem. Phys.* **1993**, *98*, 5648. (b) Lee, C. T.; Yang, W. T.; Parr, R. G. *Phys. Rev. B* **1988**, *37*, 785.

- (46) (a) Perdew, J. P.; Yue, W. *Phys. Rev. B* **1986**, *33*, 8800. (b) Perdew, J. P. *Phys. Rev. B* **1986**, *33*, 8822.
(47) (a) Schäfer, A.; Horn, H.; Ahlrichs, R. *J. Chem. Phys.* **1992**, *97*, 2571. (b) Schäfer, A.; Huber, C.; Ahlrichs, R. *J. Chem. Phys.* **1994**, *100*, 5829.
(48) Schöneboom, J. C.; Neese, F.; Thiel, W. *J. Am. Chem. Soc.* **2005**, *127*, 5840.
(49) Molekel, *Advanced Interactive 3D-Graphics for Molecular Sciences*; available at <http://www.cscs.ch/molekel/>.
(50) Sinnecker, S.; Slep, L. D.; Bill, E.; Neese, F. *Inorg. Chem.* **2005**, *44*, 2245.